Journal of Hydrology 609 (2022) 127763

Contents lists available at ScienceDirect

Journal of Hydrology

journal homepage: www.elsevier.com/locate/jhydrol

Review papers

Hydraulic modelling of inland urban flooding: Recent advances

Emmanuel Mignot [a,*], Benjamin Dewals [b]

[a] University of Lyon, INSA Lyon, CNRS, LMFA, Ecole Centrale Lyon, Université Claude Bernard Lyon 1, UMR5509, F-69621 Villeurbanne, France
[b] Hydraulics in Environmental and Civil Engineering (HECE), University of Liège (Uliège), Belgium

A B S T R A C T

This review provides a synthesis of advances in our understanding of urban flood processes and their modelling over the last four years (2018–2021). Four aspects are covered: knowledge of urban flood flow and transport processes, stability of humans and objects within flooded streets, reliability of computational modelling and approaches for speeding-up computations of urban flood event. New laboratory setups have shed light on previously unexplored processes such as flow intrusion into buildings or contaminant exchanges between surface and underground drainage. The stability of a single pedestrians or object (e.g., vehicles, waste containers) under urban flooding was analysed, but not group effects such as clogging. Improvements in computations were achieved by new strategies for merging and processing various sources of high quality topographic and forcing data (e.g., precipitation), the incorporation of more and more details on the drainage systems (e.g., effect of gullies), and 3D instead of 2D simulations. Computational efficiency was enhanced based on massive parallelization, adaptive mesh, porosity models, surrogate models as well as machine learning. Finally crowd-sourced data are shown to offer an avenue for next generation model validation methods. Remaining knowledge gaps and guidance for future research are proposed and predict that additional research work will be performed in following years.

1. Introduction

Managing urban flood risk is a high priority worldwide, as suggested by the large number of cities, from all continents, taken as case studies in recent research papers dedicated to urban flood modelling. More than half of the global population lives in urbanized areas, and the frequency as well as intensity of hydro-meteorological extremes are on the rise (EEA, 2019; Hirabayashi et al., 2013). In inland urban areas, the invading water may originate from a combination of local precipitations, overflowing urban rivers, surcharging drainage system, and runoff from upstream (Bulti & Abebe, 2020). In coastal areas, urban flooding may additionally result from high tides, storms, tsunamis, or effects of rising sea level. In the following, the focus is mainly set on floods taking place in inland urban areas.

Urban flooding involves complex flow phenomena, which vary rapidly in space due to the multiple flow paths typical of urban areas (Rubinato et al., 2020). When water is conveyed in streets, local head losses are created by the presence of obstacles such as vehicles or urban furniture, as well as by the interplay between the drainage system and surface flow. Flow features are particularly intricate at crossroads, and other configurations such as when water invades open areas (courtyards, parks…), enters buildings (e.g., through damaged doors or windows) and large underground areas (malls, metro stations…), or follows unusual flow paths resulting from the layout of obstacles present in urbanized areas. Moreover, rapid urban flooding, such as induced by flash floods, leads to complex transient effects, as well as to the transport of debris and objects (e.g., vehicles, containers, urban furniture) (Martínez-Gomariz et al., 2018).

Computational modelling of these flow and transport processes is instrumental for guiding urban flood risk management. However, such modelling remains challenging, not only due to the variety of processes at stake and the complexity of urban topography but also because of the broad range of expected outcomes, such as predicting the loads acting on buildings or pedestrians, the drift of vehicles or urban furniture, the bidirectional flow exchanges between drainage system and surface flow, or the dispersion of contaminants (Mignot et al. 2019). Moreover, computed flow variables must reach the right level of accuracy to serve as suitable inputs for complementary analyses, such as damage modelling (Mei et al., 2020), sediment transport and morphodynamic modelling (e.g., scour prediction).

An additional challenge lies in the scarcity of observational data for the verification of urban flood computations. Indeed, such data remain mostly limited to water marks on building facades, registered by visual inspection shortly after the flood event (Macchione et al., 2019a). This approach leads to a lack of suitable calibration and validation data, especially in terms of velocity fields, time-dependent hydraulic data, and accidental events such as sudden sewer overflows, building intrusions and damages, dams created by cars blocked at a crossroad or a street narrowing. The increasing use of smartphones and of videos by citizens is a new paradigm for harvesting validation data and much current

* Corresponding author.
E-mail address: Emmanuel.mignot@insa-lyon.fr (E. Mignot).

https://doi.org/10.1016/j.jhydrol.2022.127763
Received 28 January 2022; Received in revised form 15 March 2022; Accepted 21 March 2022
Available online 25 March 2022

Table 1
Research topics associated to urban flooding, and their coverage in the present review.

	Domains or topics	Objectives	Covered (C) Partially covered (PC) Not covered (NC)
Quantification of water volumes entering urban areas	Meteorology	Predict the rain distribution over the urban areas	NC
	Hydrology	Predict the runoff discharge from upstream catchments	
	Fluvial hydraulics	Predict river overflows upstream or within the urban areas	
	Urban hydrology	Predict sewer overflows: locations and hydrographs	
Describing the city (topography)	Topography – GIS	Improve the quality of urban domain description.	C
	Algorithmic (computer sciences)	Accelerate / automatize mesh construction …	NC
Flow patterns within the urban area	Open-channel hydrodynamics	Better understand and model floods at the surface of urban areas	C
	Pressurized flows	Better understand and model flows in the sewer systems	NC
	Sewer – surface flow exchanges	Predict sewer-surface exchange discharges and effects on surface flow	C
Validation data (e.g., flood marks …)	Social medias, image analyses	Get reliable validation data	C
Vulnerability and risk	Experiments	Establish stability curves for humans and furniture	C
	Economy	Predict direct and indirect damage	NC
	Flood preparation	Improve early-warning, rescue planning, crisis management	NC
	Mapping	Generate risk map to prepare rescues, evacuation, alternative routes…	PC
	Communication, policy support …	Transfer information to citizens, stakeholders, decision makers	NC
Resilience	Social sciences	Evaluate strategies to go back to normal as fast and efficient as possible	NC

research is dedicated to extract reliable information from amateur videos and crowd-sourced data (Moy de Vitry et al., 2019).

Modelling urban flooding is a relatively recent field of research. Indeed, although urban floods and their impacts have been reported for centuries (e.g., since the XIV century in the city of Nîmes, France), research dedicated to the understanding and modelling of urban flooding remained scarce until the beginning of the 21st century. Beforehand, pioneering contributions were made by Braschi et al. (1989), Kinoshita et al (1996), Nania (1999), Djordjevic et al. (1999) and Heping et al. (1999). Conversely, the past 20 years showed a dramatic increase in the number of experimental and computational studies on this topic (e.g. Mignot et al., 2019; Guo et al., 2021a; Rubinato et al., 2020). Over the last four years (2018–2021), we identified more than sixty peer-reviewed journal papers presenting substantial advances in the understanding of flow processes and modelling capacity of urban flooding in inland areas. Due to this high number of new contributions, the present synthesis is deemed valuable for the community. By focusing on the most recent contributions, it provides both an update and a complement to previous, more specific syntheses restricted generally either to laboratory experiments (Mignot et al., 2019) or to computational models (Bulti and Abebe, 2020; Guo et al., 2021a; Nkwunonwo et al., 2020). Studies based solely on the application of existing modelling techniques to case studies were not incorporated in this review.

As detailed in Table 1, the scope of the present review targets the specific features of flooding in urban areas. In contrast, it does not aim at covering general aspects of flood modelling and prediction, which are not tightly linked to the urban nature of the exposed area. Therefore, this review does not include studies on rainfall prediction nor on catchment hydrology and fluvial hydraulics in general (e.g., Brunner et al., 2021). While the quality of accessible topographic data required for urban flood modelling lies in the scope of the review; we do not report developments in data processing algorithms nor purely technical advances such as in geographic information systems (GIS). Similarly, the review extends up to the interface between flow modelling and complementary analyses, such as economic damage assessment, decision-support systems, or resilience studies; but it does not cover these complementary analyses themselves. Green infrastructures (e.g., Fowdar et al., 2021) are also considered beyond the scope of the present review, in which the focus is set on the hydraulic mechanisms involved in urban flooding.

The review is organized in two main sections. Section 2 summarizes recent research works on understanding urban flood flow processes and vulnerability factors, derived both from experimental and numerical approaches. Section 3 presents advances in numerical modelling of urban flooding, aiming either at enhancing the accuracy of computational predictions (Section 3.1), or at speeding up the computations (Section 3.2). Fig. 1 provides an overview of the number of studies reviewed in each section of this paper. Finally, a discussion and concluding remarks are given in Section 4.

2. Physical understanding of urban floods and associated vulnerability

2.1. Flow processes

Mignot et al. (2019) reviewed the experimental studies and datasets published before 2018, aiming at advancing our understanding of flow processes during urban flooding, such as flows at crossroads, in street networks and urban districts, as well as flow exchanges between surface and urban drainage systems. Table 2 summarizes 19 more recent studies pursuing the same goal. Most of them involve laboratory experiments which also deliver quantitative, well documented data of high value for validating current and new computational models.

In Table 2, the studies are classified according to the modelling approach (experimental vs. computational), the extent of the considered domain (single street vs. urban district, including or not urban drainage pipes), the source of water (from rain over the studied domain, runoff over the upstream catchment, or from the surcharged urban drainage system) as well as the type of analysed data (discharge partition in street networks or at manholes, flow depths and velocities). As detailed below, six laboratory setups reported here are totally new and were not

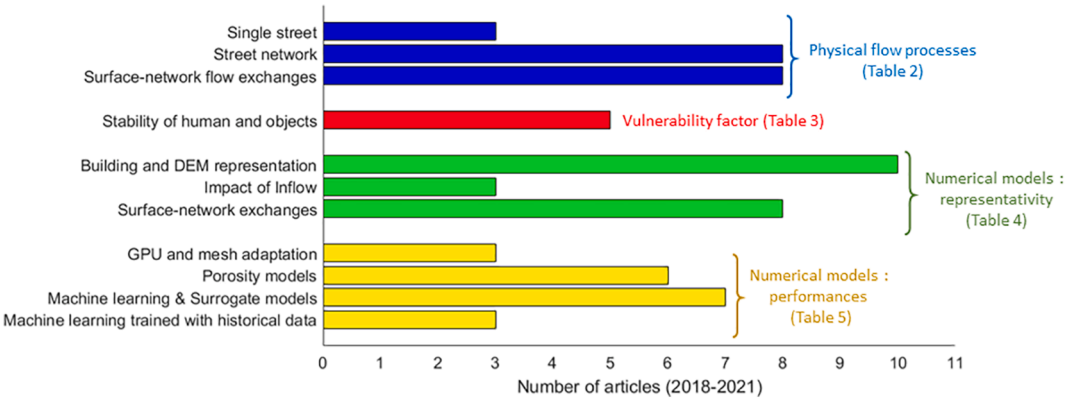

Fig. 1. Statistics of papers dedicated to urban flow modelling, published over the period 2018–2021.

included in the previous review by Mignot et al. (2019).

Several recent studies focused on the prediction of flow exchanges between surface and urban drainage. At the Technical University of Catalonia (Barcelona, Spain), Gómez et al. (2019) used a laboratory platform representing a road lane at prototype scale to estimate orifice discharge coefficients through an urban drainage inlet, under surcharging sewer flow conditions. The coefficients were found not to vary with the road slope. Based on a new experimental setup at the University of Wuppertal (Germany), Kemper & Schlenkhoff (2019) developed an empirical formula to estimate the type-specific hydraulic capacity of grate inlets with supercritical surface flows. The experiments represent a single steep-sloped street, with water supplied upstream. The parameters influencing the grate inlet capacity are the flow depth and velocity upstream of the grate as well as the grate characteristics (dimensions and orientation of the bars).

In contrast with the tests performed by Gómez et al. (2019) and Kemper & Schlenkhoff (2019), other recent experiments include an explicit representation of urban drainage pipes in the laboratory. Four recent studies are based on an experimental setup installed at the University of Sheffield and already reported by Mignot et al. (2019). The setup is a 1:6 scale representation of a single street linked to a single urban drainage pipe by a manhole. Rubinato et al. (2018b) measured the inflow discharge into the manhole under steady surface inundation conditions. Weir and orifice discharge coefficients were determined for a range of grate designs, and a 2D finite difference model was validated in terms of simulated flow depths around the inlet. With a 2D surface particle image velocimetry technique, Martins et al. (2018a) measured, for the first time, details of the velocity field in the vicinity of the manhole, with ten different grate designs. Only drainage flow was considered, under subcritical surface flow conditions. A 2D numerical model was also assessed. Rubinato et al. (2018a) quantified energy losses within the manhole for surcharging and non-surcharging outflow conditions. The tests enabled evaluating the influence of a manhole lid and of a shallow flow on the surface, as well as validating a computational model. Beg et al. (2020) used the same experimental setup to quantify flow and solute mass exchange through the manhole, with the aim of better understanding how pollutant is released from the sewer network to the street surface during urban flooding. In the same experimental facility, Rubinato et al. (2021) considered a variety of street configurations (involving parking slots, cars on the road and various locations of the manhole on the street), to generate a novel dataset covering flow exchanges, energy losses and quantification of exchanges of soluble pollutant from the sewer to the surface during urban flooding.

Dong et al. (2021) used a new laboratory setup at North China University of Water Resources and Electric Power. It consists in a 16-m long and 3-m wide model of a single street, with an urban drainage pipe underneath. In their tests, Dong et al. (2021) analysed the influence of varying the number of buildings and the spacing in-between them on the flow generated by a dam-break at the street inlet. Hydrographs, flow depths and velocities were recorded in unsteady conditions at several points, and the predictions of a 2D finite volume model were compared to the observations. Another new setup, at INRAE (Lyon, France), was used by Chibane et al. (2021). In its present form, it involves a single street connected to a single urban drainage pipe by means of up to two drains, and it was used for evaluating the influence of the flow exchange, both under drainage and surcharged configurations, on the 3D velocity field and water depth in the street near and downstream from the connections. This new dataset is valuable to validate numerical models including vertical exchange flows through manholes.

Another research topic which was hardly explored in the past is the quantification of water intrusion into buildings (Zhou et al., 2016; Liu et al., 2018; Sturm et al., 2018) during urban floods. A new experimental dataset collected at INSA Lyon (France) is presented by Mignot et al. (2020). It was obtained using a scale model of a single building façade with various openings (door, window, gate). Conducted measurements include the discharge partition between the street and through the façade along with flow depths and velocity fields in the street. The novel experimental facility used by Chibane et al. (2021) was also used by Mejía-Morales et al. (2021) under another configuration to study, at reduced scale, flood flows in the vicinity of an urban block surrounded by four streets. The number and positioning of door-like openings along the faces of the urban block were varied, and their influence was assessed in terms of exchange flow with the streets, flow depth and velocity in the streets and in the block, as well as danger for pedestrians. Notable effects were found in the near field of the openings.

While all studies mentioned above are based on laboratory setups representing at most four streets (with or without a single conduit underneath), Finaud-Guyot et al. (2018; 2019) investigated the discharge partition in a 1:200 scale model of an urban district (14 streets), which was already analysed earlier by Arrault et al. (2016). Due to the multi-scale nature of urban flooding at the district level, the scale model of Finaud-Guyot et al. (2018; 2019) was geometrically distorted, i.e., the scale factor along the vertical direction is ten times lower than the horizontal one. This approach was also used in earlier studies of urban flooding (e.g., Güney et al., 2014; Haltas et al., 2016a; b; Smith et al., 2016). The possible bias induced by this geometric distortion was studied by Li et al. (2019). The effect of geometric distortion of scale models of urban flooding was further analysed by Li et al. (2020; 2021) based on a comprehensive series of numerical computations and dedicated laboratory tests on a new experimental set-up.

Seong et al. (2020) used a new 1:200 scale representation of an urban district in Sadang (South Korea). Unlike all other experiments mentioned above, water was supplied to the scale model by means of a

Table 2
Improvements in knowledge of physical processes involved in urban flooding, based on experimental or numerical studies.

	Type		Studied domain				Water origin			Type of data				
	Experiments	*Computations*	*Single street*	*District*	*Urban drainage network*	*Single urban drainage pipe*	*Surface runoff from upstream*	*From the sewer network*	*Local rain*	*Velocities*	*Water depths*	*Discharge*	*Other*	**Scientific question**
Gomez et al. (2019)	X		X					X			X	X		How the sewer overflows to the street through a manhole with grids?
Kemper & Schlenk-hoff (2019)	X		X				X					X		How the rapid flow in the street flows down through inlets towards a sewer conduit?
Rubinato (2018b)	X	X	X			X	X				X	X		How much drainage water flows through a manhole covered by different grates with the aim to quantify drainage discharge coefficients?
Martins et al. (2018a)	X	X	X			X	X			X		X		How the street flow enters a sewer through a manhole? Measured surface velocities around the manhole are useful to validate numerical models
Rubinato (2018a)	X	X	X			X	X	X			X		Pressures	How much head is lost at the connection between a conduit and a manhole (with/without surcharged manhole, with/without a lid, with/without initial water at the street surface)?
Beg et al (2020)	X	X	X			X	X	X		X		X	Concentrations	How concentration and mass of sewer flow spreads in a manhole and is distributed between the downstream conduit and towards the street surface?
Rubinato et al. (2021)	X		X			X	X	X				X	Pollutant discharge	How much pollutant is passed from an overflowing sewer towards a flooded street with different geometrical characteristics?
Chibane et al. (2021)	X		X			X	X	X		X	X	X		How the exchange flows from the sewer to the street through manholes affect the velocity field and water depths in the street?
Dong et al. (2021)	X	X	X			X	X			X	X	X		How a dam-break upstream a single street connected (or not) to a conduit underneath and including (or not) impervious buildings generates a complex flow along the street and towards a sewer conduit through manholes?
Mignot et al. (2020)	X		X				X			X	X	X		How water flows from a flooded street towards an opening (door – window) included in a building façade? And what is the influence of urban furniture on the intrusion discharge?
Chibane et al. (2018)		X		X	X		X	X		X	X			How the flow behaves in a fully coupled simplified surface / sewers network?
Finaud Guyot et al. (2018)	X			X			X					X		How the discharge partition towards the downstream streets of an urban district evolves as a function of the inflow distribution?
Finaud Guyot et al. (2019)	X			X			X			X	X	X		How the surface street flow propagates in a street district? A new method to measure the street discharges is proposed
Mejía-Morales et al. (2021)	X			X			X			X	X	X	Risk level	How openings in a building block affect the hydrodynamics and risk level in the block and surrounding streets
Li et al. (2019)	X			X			X			X		X		How the geometrical distortion of urban flood experiments affects their representativity?
Li et al. (2020)		X		X			X			X		X	Flow separations	
Seong et al. (2020)	X			X					X	X	X			How rain falling over a district flows in the street network towards downstream? And challenge to measure water depth and flow velocities underneath falling rain.
Bruwier et al. (2018)		X		X			X				X			How does the urban layout influence the inundation flow? Which arrangements of new buildings are preferable for flood-proof urban planning?
Bruwier et al. (2020)		X		X					X		X	X		

rainfall simulator with an intensity ranging between 80 and 200 mm/h. Intricate measurements of flow depth and surface velocity were performed under falling rain. For similar pluvial flooding conditions, Bruwier et al. (2020) investigated computationally the influence of the layout of buildings in a synthetic urban area on flow variables such as the flow hydrograph at the outlet of the considered urban district as well as the evolution of flow depths. Bruwier et al. (2018) performed the same type of analyses for the case of flood water originating from upstream drainage or river overflow, instead of local rain.

Overall, these recent pieces of research aiming at improving our knowledge of flow processes in urban flooding tackle both previously studied processes (e.g., water exchanges between surface and underground drainage system, flow partition within a network of streets) and newly explored processes, such as the flow intrusion towards a building (Mignot et al., 2020), the effects of geometric distortion on street flows (Li et al., 2019; 2020) and the release of contaminants by a surcharging sewer (Beg et al., 2020; Rubinato et al., 2021). Still, in line with the list drawn by Mignot et al. (2019) in their Table 2, other gaps in existing data remain, such as the flow processes in a street network in supercritical regime, flow exchanges between a network of streets and a network of pipes (Chibane et al., 2018), or pollution, furniture and trash dispersion in a street network.

2.2. Stability of humans and objects

Results from hydraulic modelling are often used to predict the stability of pedestrians during urban flooding, as this information is of utmost importance for planning safe evacuation routes and rescue operations. Empirical closures are needed to assess pedestrians' stability based on computed flow variables. While such closures have been proposed for over a decade (e.g., Kvocka et al., 2016; Martínez-Gomariz et al., 2016), they were further improved over the last few years with new measurement campaigns, as shown in Table 3. Postacchini et al. (2021) developed a novel laboratory approach, in which a physical model of a human body is towed by an engine in water at rest, and hydraulic forces and moments applied on the body are measured. According to the measurements, conducted for a range of flow depth and velocity, the stability condition differs substantially whether the body front or the body back faces the flow. This contrasts with previous research, in which both positions were considered similar as regards pedestrian stability. Based on a re-analysis of field measurements during a major flood event in Brisbane (Australia), Chanson and Brown (2018) suggested that the influence of local topographic effects and debris was underestimated in previous research, leading to unsafe assessment of the stability of pedestrians. They proposed new, more conservative guidelines.

However, simulations of safe evacuation during urban flooding requires not only stability criteria, but also estimates of the speed of motion of individuals in flowing water (Baba et al., 2017). Recently, Bernardini et al. (2020) involved >200 volunteers in laboratory experiments of evacuation in still water. Their results enable quantifying the speed of isolated pedestrians as a function of flow depth and body characteristics, such as age, height, and mass. The results highlight that fire or general-purpose databases of evacuation speed should not be used for analyses in floodwaters, due to a strong reduction of speed induced by water forces.

Evaluating the stability of vehicles during urban flooding is also of paramount importance, not only because drifting vehicles may endanger pedestrians or rescue services, but also because the number of people perishing in vehicles made unstable by floodwaters is reported to grow globally. Complementing earlier experimental works (Martínez-Gomariz et al., 2017; 2018), Smith et al. (2019) present a novel series of tests using full-scale vehicles. Various flow depths, buoyancy conditions, vehicle types and bed surface (concrete, gravel, or sand) were tested. The observations were combined with measurements in smaller scale laboratory tests to derive stability criteria applying to a broad range of vehicles. In a recent review, Bocanegra et al. (2020) highlighted the need for improvement and standardization in the vehicle stability criteria used across various studies.

During urban flooding, pedestrians also face the danger of being hit by drifting urban objects (urban furniture, trash etc…) such as waste containers which are used in many cities worldwide. Martínez-Gomariz et al. (2020) derived new stability criteria for waste containers based on an analytical model and proposed adaptation measures. Note that waste containers made unstable may lead to street damming and are likely to induce environmental and health risks due to contaminated material possibly released in the floodwaters.

The stability of single pedestrians, vehicles, or other objects such as waste containers is today comprehensively assessed, and lead to formally similar expressions in terms of flow depth and velocity. Data which remain missing concern mainly group effects such as: (i) several objects (vehicles, containers or other) made unstable, transported, and possibly clogging a street or a narrow path; (ii) stability and speed of motion of several interacting pedestrians, typically evacuating towards shelters. Moreover, most tests reported above were conducted under controlled experimental conditions (even if performed at full scale), so

Table 3
Improvements in stability analyses.

	Elements			Approach			Representativity			Short description
	Pedestrians	Cars	Trash containers	Experiments	Analytical	Field	Real bodies	Dummy	Small scale	
Postacchini et al. (2021)	X			X				X		Stability of real scale humanoid model facing the flow or backward.
Chanson and Brown (2018)	X					X	X			Reanalysis of pedestrian stability curves based on field data collected during an urban flood in Brisbane in 2011
Bernardini et al. (2020)	X			X			X			Flume experiments of evacuation capacities by running or walking under various conditions
Smith et al. (2019)		X		X			X		X	Real scale and small-scale car stability in water
Martínez-Gomariz et al. (2020)			X		X		X			Analytical force and torque balances to reach drag coefficients and establish stability functions of trash containers

that the derived criteria still need verification in real-world conditions, as conducted by Chanson and Brown (2018) for the case of pedestrians.

3. Computational models

Validated computational models are particularly valuable for guiding disaster risk reduction strategies in practice. They permit both to reproduce historical events for which validation data is available and simulate scenarios for various return periods and anticipating changes in climate conditions and land use. Several reviews of urban flood modelling were recently published by authors such as Bulti and Abebe (2020), Guo et al. (2021a) and Nkwunonwo et al. (2020). Rosenzweig et al. (2021) recently listed remaining challenges of such modelling, notably with respect to:

- access to input data (e.g., sewer system, location of buildings, topography from GIS databases, precipitation data…)
- processing of data (e.g., building treatment method, …)
- coupling method of overland flow models (e.g. with sewer pipe system, groundwater model, green infrastructure…)
- access to validation data for historical events (e.g. in-situ measurements, crowdsourcing and flow characteristics within the sewer network)
- translate hydrodynamics results, in terms of flow variables (flow depths, flood extent …), to damage and/or risk data and maps…

The 40 reviewed novel contributions are classified into two categories. First category deals with efforts made to improve the agreement of simulations outcomes with reference data (Section 3.1); second category deals with efforts aiming at reducing the runtime of computational models or increasing the domain size (Section 3.2). Some overlap exists between the two categories, since in the latter the pursued objective is generally to reach an optimal balance between computational efficiency and accuracy.

3.1. Improving urban flood numerical simulations accuracy

Recent contributions aiming at improving the ability of urban flood computational models to match observations were structured along four main groups in Table 4. First, a lot of attention was paid to the influence of topographic data, including digital elevation model (DEM) and building treatment methods (BTM), as well as their processing (e.g., merging various data sources). The influence of landcover data resolution and roughness parametrization was also studied. A second group of papers analysed the effects on model outputs of characteristics and spatial distribution of forcing inputs (boundary conditions) such as rainfall or inflow hydrograph. In the third group, the influence of sewer flow modelling was evaluated, particularly as regards the numerical representation of the modelling interconnections between overland flow and sewer flow. Finally, a fourth group of studies aimed at collecting more validation data, including non-conventional data, and improving their quality. Recent contributions along these four lines are detailed in the following paragraphs.

3.1.1. Digital elevation model (DEM) and building treatment method (BTM)

Several recent studies focused on the representation of buildings in the computational model. Schubert & Sanders (2012) defined three standard building treatment methods: the building resistance (BR) method, in which a high local roughness is assigned to the cells occupied by buildings; the building block (BB) method, in which the topography is raised up to the roof level over the building footprint; and the building hole (BH) method which excludes the footprint of the buildings from the computational domain.

Using a 2D shallow-water model, Mustafa and Szydłowski (2021) compared the BR and BB methods for predicting time series of pointwise water levels in a reduced-scale experiment representing a hypothetical network of buildings flooded by a dam break wave. They highlighted a strong sensitivity of the model outcomes to the value of the roughness parameter assigned to the buildings in the BR method and the superiority of the BB method for simulating realistic flow fields within an urban area.

Bermúdez & Zischg (2018) performed a similar comparison by considering also the BH method and extending their analysis to the effects of the building treatment method on damage estimation at the micro-scale (building) level. For a real-world case study covering an area of about 5 km^2 close to Bern (Switzerland), they found that the building treatment method had little effect on exposure (i.e., number of elements at risk which depends on flood extent), but a substantial influence on the flow depth attributed to each building. Among the tested methods, attributing the maximum flow depth of all nodes within the building footprint and a specified buffer distance to the building showed robust results, in the sense that it reduced the influence of the building treatment method on damage estimates.

Considering a pluvial flooding event in 2016 in Wuhan (China), Shen et al. (2018) tested a different building representation. In their approach, ground surface elevations are raised by the building entrance height, compared to nearby ground level, and a high value of roughness coefficient is assigned to areas within the building footprints to account for resistance due to inner walls. They report an improved model performance. For the same case study, Shen & Tan (2020) showed that a high-resolution resampling of the DEM close to buildings improves the computations.

The influence of DEM resolution (17, 35 and 70 m) and representations of buildings and roads was also investigated by Geng et al. (2020) for the case of pluvial flooding (2 and 10-year design storms) in a densely urbanized district of Nanjing (China). The BB method was compared to an alternate approach in which the elevation of roads was reduced by a predefined value, corresponding to a standard kerb height, so that roads act as shallow drainage channels. In the considered case study, the terrain resolution had a stronger influence on the accuracy of flow depth and flood extent estimates than the representation of buildings and roads.

Considering the overwhelming influence of topographic data and the uncertainties affecting such data, recent studies emphasized the value of merging several data sources. For a small urban area (2.8 km^2) in Italy, Arrighi & Campo (2019) compared flood extents, flow depths and building-level damage estimates using four DEMs constructed based on: raw data from a LIDAR survey, raw data with building footprints filled by linear interpolation of terrain elevations, raw data with BB method and the same merged with additional elevation data surveyed in the field. Local differences between DEM data and field-surveyed elevation points were generally small (0.26 m bias) but reached up to 2.5 m locally. An assimilation technique was used to merge the two data sources (LIDAR and field survey) weighted by the inverse of their uncertainties. In the considered case study, the data merging brought limited improvement due to the limited differences between the two datasets. Along the same line, Leitão & de Sousa (2018) assessed the influence on modelling results of various methods for merging airborne LiDAR and UAV photogrammetry data. They provide evidence for the necessity of advanced merging techniques, which take into consideration the systematic inaccuracies of the individual datasets. This was found particularly important when the merging boundaries are parallel to the contour lines.

Topographic data resampling techniques generally used to avoid excessive simulation runtimes often result in blurred representation of small-scale urban and topographical features (e.g., narrow paths between buildings are incorrectly represented). To address this issue, Ramsauer et al. (2021) implemented virtual surface links between buildings to mimic the flow paths of a high-resolution model. When applied to a synthetic rainfall case study, the virtual surface links demonstrated a substantial improvement, but the magnitude of the

Table 4
Improvements in processes representation in urban flood numerical simulations (Zhang et al., 2021b).

Reference	Focus of the study[1]	Water origin	Model type[2]	Model(s) name(s)	Computational domain	Case study	Analysed variables
Mustafa & Szydłowski (2021)	BTM	Upstream hydrograph	OFM	HEC-RAS 2-D	From 3,641 to 92,403 cells	Laboratory tests	Pointwise water level evolution
Bermúdez & Zischg (2018)	BTM	Upstream hydrograph	OFM	Iber	4.8 km^2 10^6 cells	Real-world area, synthetic flood wave.	Flow depth, damage
Shen et al. (2018); Shen & Tan (2020)	BTM, DEM	Local rain	Coupled SFM and OFM (hydro-inundation)	SWMM, LISFLOOD-FP	1.96 km^2 Grid spacing from 5 to 30 m	Real-world event	Flow depth
Geng et al. (2020)	BTM, DEM, road treatment	Local rain	Coupled SFM and OFM	MIKE 21	~ 30 km^2 Grid spacing from 17 to 70 m	Real-world area Design storms	Flow depth
Arrighi & Campo (2019)	BTM, DEM merging	Upstream hydrograph	OFM	TELEMAC-2D	2.8 km^2 Grid spacing = 1 m	Real-world area, Synthetic flood wave	Flood extent, flow depth, damage
Leitão & de Sousa (2018)	DEM merging	Local rain	Cellular automata	CADDIES	0.9 km^2 Grid spacing = 0.5 m	Real-world area Design storm	Flow depth and field, danger
Ramsauer et al. (2021)	DEM, virtual surface links	Local rain	Coupled SFM and OFM (hydro-inundation)	SWMM, P-Dwave 2D	~ 3 km^2 Grid spacing from 2 to 10 m	Real-world area Synthetic rainfall	Flow depth and velocity, damage
de Almeida et al. (2018)	DEM	Upstream hydrograph	OFM	-	Extreme-fine resolution: Grid spacing = 0.1 m	Real-world area Synthetic flood wave	Flow depth
Yalcin (2020)	DEM, land cover data, cell size	Upstream hydrograph	OFM	HEC-RAS 5.0	0.96 km^2 $2.4x10^6$ cells	Real-world area Synthetic flood wave	Flow depth and velocity, arrival times
Rong et al. (2020)	DEM	Storm surge	3D flow model, and OFM	-	2.25 km^2 3×10^6 cells (2D) 66×10^6 cells (3D)	Real-world event	Flow depth and velocity, damage
Paquier et al. (2020)	Effect of rainfall distribution and boundary conditions	Local rain	OFM	Rubar20	~ 4 km^2 ~ 10^5 cells	Real-world events	Flow depth and velocity
Mei et al. (2020)	Effect of design storm characteristics	Local rain	OFM (hydro-inundation)	Telemac 2D	143 km^2	Real-world area Design storm	Flow depth, damage
Chen et al. (2018)	Effect of boundary conditions and friction	Steady inflow	OFM	Telemac 2D	$4x10^5$ cells	Laboratory tests	Flow depth
Anni et al. (2020)	Modelling of sewer network and soil characteristics	Local rain	Coupled SFM and OFM	MIKE URBAN	3.9 km^2	Real-world event and design storms	Flow depth
Jang et al. (2018; 2019)	Modelling connections between surface and sewer	Local rain	Coupled SFM and OFM	Model by Hsu et al. (2000)	19 km^2 Grid spacing = 5 m	Real-world event	Flow depth, surface-sewer exchange
Chang et al. (2018)	Modelling connections between surface and sewer	Local rain	Coupled SFM and OFM	SWMM 4.4	400,000 cells	Real-world events	Flow depth
Hao et al. (2021)	Modelling connections between surface and sewer	Local rain	Coupled SFM and OFM (hydro-inundation)	FullSWOF-2D, SWMM 5.1	0.47 km^2 Grid spacing = 5m	Full-scale experiment, and real-world event	Flow depth, surface-sewer exchange
Zhang et al. (2021b)	Connections between sewer and surface nodes	Local rain	Zero-inertia OFM, with SFM	DHMUrban	0.35 km^2 Grid spacing = 5m	Real-world event	Flow depth, flooding time
Martins et al. (2018)	Type of sewer model	Local rain	Coupled SFM and OFM	GWM, SWMM, SIPSON	0.18 km^2 ~ 45,000 cells	Real-world area Design storm	Flow depth, damage, surface-sewer exchange
Quintana-Romero & Leandro (2021)	Types of sewer and overland flow models	Local rain	Various settings of SFM and 1D or 2D OFM	SWMM (1D), P-Dwave 2D	49.45 km^2 Various discretizations	Real-world event	Flow depth, outflow volume
Sämaan et al. (2019)	Pollutant transport from sewer to street	Local rain	Coupled SFM and OFM, with Lagrangian transport model	HYSTEM EXTRAN 2D	6 km^2 1.2 million cells	Synthetic area	Flow depth and velocity, sewer exchange, pollutant concentration

[1] BTM stands for building treatment method; DEM for digital elevation model; [2] OFM stands for 2D overland flow model (shallow-water type); "hydro-inundation" model refers to OFM also incorporating a rainfall-runoff module, i.e., modelling infiltration. SFM stands for 1D sewer flow model. Coupled SFM and OFM are commonly named *dual drainage* models.

improvement primarily depends on the size, density, and arrangement of the buildings in each specific floodplain.

Using extremely fine-resolution terrain data (10 cm) in an urban-flood case study in the UK, de Almeida et al. (2018) demonstrated that decimetre-scale alterations in the elevation of streets can lead to remarkable differences in predicted flow data. On one hand, this makes urban flood modelling challenging since such small-scale topographic details are rarely available for practical engineering studies and considering them would lead to prohibitive computational costs. On the other hand, slight alterations in the topography at tactically selected locations proved sufficient to guide flow to low impact zones (e.g., parks) and away from key vulnerable assets. This creates new opportunities for flood mitigation. However, such conclusions seem case-specific and strongly dependent on the studied events and topography of floodplains, as suggested by Yalcin (2020) who comes to conclusions somehow contrasting with those of de Almeida et al. (2018). For the case of an urban floodplain in Kirsehir (Turkey) affected by a 500-year flood scenario, Yalcin (2020) compared 19 combinations of resolutions used for DEM (0.04 to 10 m), Manning roughness layer (2 to 25 m) and computational grid (2 m to 25 m). The computations with 10 m cell size performed similarly to the very fine resolution, so that very-fine resolution of topography and high resolution landcover were judged unnecessary in the tested case.

In a game-changing contribution, Rong et al. (2020) demonstrated the potential of 3D computational fluid dynamics, compared to conventional 2D approaches. For a flooding case study in a coastal city due to storm surges, data inferred from digital aerial photogrammetry enabled reproducing more realistic flow patterns than when the 3D flow model is combined with a standard DEM, particularly in the presence of narrow streets and complex topographic features, or when a 2D flow model is used. Moreover, the use of building information model (BIM) combined with 3D computational fluid dynamics enables extending the flood simulation inside the buildings as the flow enters through openings.

3.1.2. *Effect of forcing inputs and friction*

Based on a depth-averaged surface flow model, Paquier et al. (2020) simulated two real-world cases in France (2000 pluvial flooding in Marseilles, and 2008 river flooding in Oulins) with the aim of assessing uncertainties arising from forcing inputs such as rainfall spatial distribution over the domain or upstream hydrograph in the river. In the first case study, rainfall distribution was found to change peak flow depths more than any other input parameter. In the second case study, flood level in the river has more influence than, e.g., the building treatment method.

Using a hydro-inundation model (i.e., surface flow model incorporating also a rainfall-runoff module), Mei et al. (2020) studied the influence of a design rainstorm on inundation and damage levels. For a field case study (Xiamen Island in China), several design rainstorms, corresponding to various return periods, asymmetry, and durations (constant volume), were compared. The authors show that, for a given rainfall volume, intensity is the key factor influencing inundated area, flow depth and direct damage to buildings, while the effect of rainfall pattern is slightly weaker.

Based on variance decomposition methods, Chen et al. (2018) conducted spatial global sensitivity analysis of shallow-water models applied to steady, subcritical flood flows in an experimental setup representing an idealized urban district. In the considered setting, flow depth variance is explained at almost 70 % by prescribed downstream flow depth, to less than 10 % by the friction coefficient, and to less than 25 % by the upstream discharge. For supercritical cases, sensitivity to friction coefficient is higher.

3.1.3. *Effect of sewer systems modelling, and interactions with surface flow*

Guo et al. (2021a) and Nkwunonwo et al. (2020) listed the numerical models available to simulate surcharging sewer networks and overland surface flows. These models are generally referred to as "*dual drainage models*" (Djordjevic et al., 1999), as they involve the coupling of a 1D sewer flow model and a 2D overland flow model. Anni et al. (2020) revealed that, for the case of a pluvial flooding event in Tuscaloosa (USA), incorporating or not stormwater infrastructures in the modelling changed the flood volumes by factors 8 to 20 depending on the return period. The same flood simulations were also sensitive to the spatial explicitness of soil input data (pervious vs. impervious). Moreover, based on comparisons with full-scale laboratory experiments and the simulation of a storm event in Beijing (China), Hao et al. (2021) stress the importance of representing bidirectional flow exchanges and initial surface runoff dynamics, while accounting for the pressure needed to lift manhole cover only marginally improves the results.

Still, a remaining major challenge for such urban flood simulations is the scarcity of data on location and characteristics of stormwater infrastructures. Bulti and Abebe (2020) analysed the necessary level of detail in representing the connections between surface flow and sewer network. Should each inlet be modelled, or does lumping the exchanges at the level of manholes provide sufficient accuracy? For the case of a high intensity storm in 2015 in Taipei city (Taiwan), Jang et al. (2018) showed that modelling individual inlets performs considerably better in terms of comparison with field observations of flood extent. Modelling not only sewer pipes but also gullies (which act as buffers between surface and sewer) further improves the agreement with field observations for the same 2015 storm and for a milder one which occurred in 1993 (Jang et al., 2019). Similar conclusions were obtained by Chang et al. (2018) by simulating three historical flood events in another district of Taipei. The extra computational time for inclusion of flow processes in gullies was deemed limited compared to the gain in accuracy.

Martins et al. (2018b) focused on the influence of the sewer flow model. By comparing four different sewer flow models for a case study in Bradford (UK), the authors found an overall good agreement between the model outcomes, with differences in estimated damage of the order of 6 %.

In a recent contribution, Quintana-Romero & Leandro (2021) compared seven model structures, involving overland flow representation by various combinations of 1D and/or 2D models, and sewer flow representation either computed using 1D models or being neglected. The results of the model structures were evaluated based on data from a 2007 flash flood in the town of Baiersdorf (Germany), characterized by a heterogeneous urban density. Several model structures performed as well as a full 1D-2D dual drainage model, and the model outcome uncertainties were found highly spatially-variable.

A Lagrangian transport model, coupled to a sewer-overland flow model (1D-2D dual drainage model), was introduced by Sämann et al. (2019) to compute the transport of solute originating from surcharged sewers, and to predict the resulting pollution spreading in streets during an urban pluvial flooding. A random walk approach was used for mixing and dispersion calculation. The impact of various simplifications in the hydrodynamic model was assessed; but no useful simplification could be recommended. Particularly, the authors showed that the flow patterns are better captured by hydrodynamic models than by simplified ones, and that a high temporal resolution of the flow field is required to reproduce short duration changes in contaminant paths.

3.1.4. *Validation data*

The scarcity of available data for model elaboration, calibration and validation is another major challenge hampering the development of flood modelling and management models (Molinari et al., 2019). To overcome this, considerable efforts were made to retrieve valuable data from unconventional sources, such as crowd-sourced data. To reconstruct hydraulic data from an urban flood event in the town of Crotone (Italy), Macchione et al. (2019a) combined amateur videos, photographs, traditional topographic surveys, news reports, among others. They proposed a methodology to merge various conventional and unconventional sources of information. Scotti et al. (2020) presented

another integrated approach for the reconstruction of temporal and spatial patterns of a flood event. For the case of hurricane Harvey in Houston (Texas, USA in 2017), they combined satellite images and markers from social media hydraulic for effectively calibrating and validating the outcomes of their hydraulic model. Authors showed that merging various data sources helps coping with the high uncertainties affecting each individual source of information. Moy de Vitry et al. (2019) used existing surveillance cameras to infer insights on the flood level evolution. Their image processing technique relies on a deep convolutional neural network, trained based on over 1,2000 flooding images. The system was deemed cheap, versatile, scalable, and transferable to other sites.

3.2. Reducing the computational time of urban flood modelling

Improving the computational performance of urban flood models is of utmost importance for a range of reasons (e.g., Bates, 2022). First, this contributes to handling larger domains, at a higher spatial resolution and/or over longer time horizons. Second, this is particularly relevant for models used not only in planning phase, but also for forecasting and crisis management purposes, since in that case model outputs are required in real-time. Various strategies are currently explored to accelerate urban flood calculations. The 19 reviewed publications were separated in four groups corresponding to four main acceleration strategies: a massive parallelization (group 1), an adaptative mesh (group 2), the use of a porosity model (group 3) and the use of surrogate models and machine learning (group 4), see Table 5.

3.2.1. Massive parallelization

Massive parallelization techniques are one avenue to speed-up urban flood calculations. The use of Graphic Processing Units (GPU) is particularly efficient as it enables leveraging thousands of processors within a single device. Based on a GPU implementation of a hydrodynamic model, Xing et al. (2019) simulated in nearly real time a flood event over a 268 km^2 urbanised area at 2 m spatial resolution, i.e., with about 67 million computational cells. By comparing model outcomes for five different spatial resolutions, the authors revealed a high sensitivity of model outcomes, due to the inability of coarser resolutions to resolve narrow flow paths (narrow rivers, small roads, and flow paths between buildings), hence reducing the connectivity in densely urbanized areas. Similarly, restricting the computation to localized subdomains introduces large simulation errors. Fernández-Pato & García-Navarro (2021) presented the first GPU implementation of a coupled dual drainage model including overland and sewer flow (along with exchanges between both models), and pollutant transport both in the sewer network and on the surface. This GPU model was applied to real-world cases, for which it led to speed-up factors of the order of 100 compared to a standard CPU computation.

3.2.2. Adaptive mesh

An alternate approach to accelerate urban flood computation consists in using a dynamically adaptive meshing technique, enabling the mesh to adapt in space and time as a function of the evolution of flow features. Hu et al. (2018) used the Hessian matrix of flow depth and velocity to adapt the mesh every 10 time steps with the algorithm Gmsh (Geuzaine & Remacle, 2009). For a real-world case study, the method provided accurate results with a computation time reduced by a factor of about 2.

3.2.3. Porosity models

Porosity models use a subgrid modelling technique to speed-up simulations of overland flow. The flow computations are performed on a relatively coarse grid, while information on the sub-grid scale topography is preserved through additional parameters, referred to as porosities (Guinot & Soares-Frazão, 2006; McMillan & Brasington, 2007; Sanders et al., 2008). These parameters reflect the effects of obstacles on storage in the cells and on flow conveyance between the cells. Alternate names have also been used for the porosity parameters, such as building coverage ratio and conveyance reduction factor (Chen et al., 2012), or area and width reduction factors (Haltas et al., 2016a; b). Porosity models are classified as “single-” or “dual-porosity” (depending on the types of considered porosity parameters), and as “differential” or “integral” (depending on their mathematical formulation). Over the last years, major improvements were brought to these models (Dewals et al., 2021).

Guinot et al. (2018) introduced depth-dependent porosities as a generalization of the dual integral porosity model, which was proposed earlier by Guinot et al. (2017) to fix erroneous wave celerities arising in the original integral porosity model of Sanders et al. (2008). To reduce the mesh sensitivity of the porosity models, Ferrari et al. (2019) tested an isotropic single porosity formulation for the fluxes, complemented by anisotropic conveyance porosities in the estimation of flow resistance. With the same objective, Viero (2019) implemented a dual-porosity model, in which the conveyance porosity is not evaluated at the cell interfaces but at the level of a computational cell. Along the same line, an algorithm for the cell-based determination of the conveyance porosity for real-world urban areas was presented by Ferrari and Viero (2020). Their approach performs well for a single obstacle in a computational cell but not in the presence of multiple obstacles. Varra et al. (2020) introduced a novel local, differential porosity model formulation, referred to as the binary single porosity model. It was derived regardless of the existence of a representative elementary volume as assumed in the derivation of earlier differential porosity models (Guinot & Soares-Frazão, 2006). The variety of approaches being currently developed emphasizes the need for further research on modelling of anisotropic conveyance effects in urban flood porosity models.

Costabile et al. (2020) systematically compared the outcomes of a single-porosity model to those of a standard fully dynamic shallow-water model, and a simplified zero-inertia model. Unlike previous model benchmarking, often restricted to comparisons of flooded extents and flow depths, Costabile et al. (2020) also evaluated the flow velocities and the product of flow depth and velocity, which is a determinant for flood impacts. The results reveal that a dynamic wave model is necessary in all situations where not only the flood extent needs to be predicted but also the flood impacts. Both the porosity model and the zero-inertia model lead to wrong estimations of the depth-velocity product.

3.2.4. Surrogate models and machine learning

Many recent studies explored radically different approaches to speed-up urban flood computations, namely machine learning. In a recent review of urban drainage models based on machine learning, Kwon and Kim (2021) point at the extensive use of such models to advance model performance and efficiency. Machine learning models are trained based on detailed hydrodynamic data, mostly water depths and velocities and can then deliver fast predictions of flow patterns over large areas for scenarios slightly departing from the configurations used for the training. Two types of machine learning approaches can be identified as a function of the origin of data used to train the model. First type considers output data from process-based numerical calculations performed for a range of input parameters (topography, boundary conditions etc…). Second type considers the data measured on-site and collected from historical events (but without any hydraulic calculation).

For the first type training data are output from hydraulic models. A binary logistic regression model, embedded in a GIS system, was presented by Feng et al. (2020) and applied to a 100 km^2 catchment in London, Ontario (Canada) with reductions in computational time by three orders of magnitude. Bermúdez et al. (2018) tested two computationally efficient surrogate models. The first one combines a detailed 1D sewer network model with a GIS volume spreading algorithm for

Table 5
Improvements in the computational performance of urban flood numerical simulations.

Reference	Acceleration strategy	Water origin	Model type[1]	Model(s) name(s)	Domain size	Simulated period	Reported efficiency
Xing et al. (2019)	GPU implementation	Local rain	OFM	HiPIMS	267 km^2 67 millions cells	28 h	Near real-time computation
Fernández-Pato & García-Navarro (2021)	GPU implementation	Various test cases	Coupled SFM and OFM, with transport model	RiverFlow2D-GPU, SWMM 5.1	0.4 km^2 ~ 10^6 cells	~ 12 h	Speed-up factors > 100
Hu et al (2018)	Dynamically adaptive mesh	Upstream hydrograph	OFM	-	0.4 km^2 Adaptive mesh	2 h	Speed-up factors ~ 2
Guinot et al. (2018)	Porosity model	Upstream hydrograph	OFM	-	Academic test cases	-	-
Ferrari et al. (2019)	Porosity model	Upstream hydrograph	OFM	PARFLOOD	Academic test cases	-	Speed-up factor > 10
Viero (2019)	Porosity model	Upstream hydrograph	OFM	2DEF	< 1 km^2 63,000 cells	2 h	-
Ferrari and Viero (2020)	Porosity model	Upstream hydrograph	OFM	PARFLOOD	< 1 km2, up to ~ 5 × 10^5 cells	2 h	Speed-up factor ~ 100
Varra (2020)	Porosity model	Upstream hydrograph	OFM	-	Mostly theoretical contributions	-	-
Costabile et al. (2020)	Diffusive wave, porosity model	Upstream hydrograph	OFM	-	3.4 km^2, up to 59,000 cells	6 h	-
Feng et al. (2020)	GIS-based model	Local rain	Binary logistic regression for overland flow	GIS model, trained based on PCSWMM	~ 100 km^2	3 h	~ 10 minutes, instead of days
Bermudez et al. (2018)	Surrogate model	Local rain	Conceptual dual drainage model	Trained based on InfoWorks ICM	27.5 km^2	6 h	Speed-up factor > 10^4
Contreras et al (2020)	Surrogate model	Local rain	Interpolation by krigging	Trained based on HEC-HMS	39 km^2 2.7 × 10^6 cells	4 h	"Instantaneous" vs. 2 days
Kim & Han (2020); Kim et al. (2019)	Machine learning	Local rain	Neural network models	NARX-SOM, trained with SWMM	1.8 to 13 km^2		Speed-up factor ~ 45
Berkhahn et al. (2019)	Machine learning	Local rain	Ensemble neural network model	ANN trained with HE 2D	3.6 km^2	Only maximum predicted	Speed-up factor ~ 10^3
Rozer et al. (2021)	Machine learning	Local rain	Neural network-based model	ANN trained with HE 2D	5 km^2	Only maximum predicted	Speed-up factor ~ 50
Guo et al. (2021b)	Machine learning	Local rain	Deep convolutional neural network	CADDIES, Infoworks ICM	-		Speed-up factor ~ 10^2 – 10^3
Wu et al. (2020)	Machine learning	Local rain	Gradient Boosting Decision Tree	GBTD trained with historical data	7446 km^2		-
Darabi et al. (2019; 2020)	Machine learning	Local rain	Ensemble of models	GARP and QUEST trained with Historical data	27 km^2		-
Lei et al. (2021)	Machine learning	Local rain	Convolutional, and recurrent neural network	$NNET_R$, $NNET_C$ trained with historical data	605 km^2	-	-

[1] OFM stands for 2D overland flow model (shallow-water type); "hydro-inundation model" refers to OFM also incorporating a rainfall-runoff module, i.e., modelling infiltration. SFM stands for 1D sewer flow model. Coupled SFM and OFM are commonly named *dual drainage* models.

overland flow. In the second approach, a conceptual lumped sewer and flood model is derived based on a blend of data-driven and physically based components, as well as pre-simulated flood maps. Both approaches provide results of comparable accuracy as a detailed hydraulic model, at a fraction of the computational cost (speed-up factor up to 10^4). Kriging was used by Contreras et al. (2020) to interpolate flow variables from a database of 49 pre-simulated scenarios, generated by means of high fidelity hydrological and hydraulic models. A critical factor to design the database is the coverage of the entire range of possible storm characteristics. Kim et al. (2019) and Kim and Han (2020) used a 1D/2D coupled model to produce the training data to learn the relationship between rainfall and overflow and inundation area resulting from manhole overflows. The database used by Berkhahn et al. (2019) and Rözer et al. (2021) for training and testing of their ANN real-time water level prediction model was generated with the 2D hydrodynamic model HYSTEM-EXTRAN 2D (HE 2D). Guo et al. (2021b) used a cellular automate and a hydrodynamic model to train deep convolutional neural networks for predicting flow depth for urban pluvial flooding.

For the second type, training data are historical measured data. Wu et al. (2020) used 14 historical rainfall and flooding records from 2013 to 2016 in Zhengzhou city (China): 11 for training and 3 for validating their machine learning model aiming at predicting flow depth maps. The most important parameters for the training are the road and building occupation ratio, the soil permeability, the grassland and forestland occupation ratios. Darabi et al. (2019; 2020) used flood historical

database obtained from Sari city authority over the period 2015–2017. Precipitation, slope, curve number, distance to river, distance to channel, depth to groundwater, land use, and elevation were used to train the machine learning model. Hydraulics data were then transferred to vulnerability maps. The authors concluded that "distance to channel, land use, and elevation played major roles in flood hazard determination, whereas population density, quality of buildings, and urban density were the most important factors in terms of vulnerability". The model used by Lei et al. (2021) was trained using the 295 locations of flooding in the city of Seoul (Korea) in the period 2018–2020, as a function of 10 flood-affecting factors. Terrain ruggedness index, bed slope, bed elevation and topographic wetness index appear to be the dominant factors to predict the inundation locations.

4. Discussions and conclusion

This review provides a synthesis of current knowledge in the understanding and modelling of urban flood processes. It is based on journal papers published over the last four years (2018–2021), and it is structured along four lines: understanding of urban flood processes, stability and evacuation, realism and accuracy of computational modelling, and speed up of computations. The review highlights the maturity of the field. Nevertheless, numerous open questions still to be addressed for improving our understanding and modelling capacity of urban flood flow processes; some examples are given below.

Currently available laboratory and field observations miss information on important flow and transport processes. Flow exchanges between sewer and surface were measured only in idealized settings involving a single street with a single pipe underneath. Observations of the interactions between a sewer network and a surface street network are still lacking. Measurements of flow intrusion inside buildings remain also limited, while such exchanges alter flow patterns in the streets and danger for pedestrians. Little is known on the dispersion in a street network of contaminants released by surcharging sewers. Similar questions exist for the particulate transport of trash, urban furniture, vehicles, and other debris.

Besides, laboratory studies have enabled assessing the stability conditions of an isolated pedestrian, vehicle, or piece of urban furniture. Verification of these results for real-world conditions remain scarce, and no information is available on group effects, such as the evacuation of a group of pedestrians from a flooded mall or metro station. The same type of knowledge gaps exists for groups of floating objects, or vehicles likely to clog narrow flow paths or singularities such as crossroads.

Improved methodologies for merging data from various sources pave the way for increasingly accurate representations of small-scale topographic features and forcings in computational models. Such methodologies are instrumental for taking full benefit of extreme high resolution (e.g., sub-metric) remote sensing data (de Almeida et al., 2018). Techniques such as GPU-based massive parallelization or machine-learning have proved successful for speeding up calculations, while theoretical advances are still needed with respect to some modelling concepts such as the incorporation of anisotropic conveyance effects in porosity-based urban flood models. For the computation of transport processes (debris, vehicles, contaminants), existing modelling paradigms (e.g., Lagrangian vs. Eulerian, 2D vs. 3D) still need to be compared among each other and with measured concentration maps to point at the most effective calculation strategies.

During urban floods, usually of short duration, collecting flow depth and velocity observations is particularly challenging. According to Macchione et al. (2019a), among the ten best documented urban flood events, three of them contain no suitable data for validating flow computations, and the others include only watermarks. The recent proliferation of mobile phones and online video sharing platforms gives access to countless amateur videos (Le Coz et al., 2016; Kankanamge et al., 2020; Zhang et al., 2021a), which are being used in most geophysical sciences. Urban floods are particularly well documented by such crowd-sourced data since they occur in densely populated areas. Moreover, the presence of urban furniture and easily identifiable geometric features of buildings facilitate the estimation of water level and surface flow velocity from image processing algorithms. Difficulties with retrieving the location and time of the scenes impairs the use of these data for detailed model validation. Surveillance cameras are another potential source of validation data even if access to recorded data by scientists is hindered by legal barriers for privacy reasons. Conversely, accessing validation data for the sewer component of dual drainage models appears much more intricate (Anni et al., 2020; Chang et al. 2018).

A particular impediment to advances in the science of urban flood modelling is that conclusions of most studies remain genuinely site-specific in their formulation. Major steps forward could be taken by attempting to extract generic knowledge from collections of existing case studies. Although challenging, this may be achieved by designing appropriate metrics for classifying and standardizing the definition of flooding scenarios, investigated processes and effects of analysed variables (e.g., model settings).

Finally, several of the reviewed studies demonstrate considerable recent efforts for translating the flow modelling results into information and data of direct use for impact assessment and risk communication. Among others, Darabi et al. (2019; 2020) and Wang et al. (2021) plotted vulnerability and risk maps, Mejía-Morales et al. (2021) used stability curves for pedestrians to draw danger maps, and Mei et al. (2020) mapped monetary damage for a range of flood frequencies. To communicate the computed flow characteristics, texture mapping techniques are used for synthesizing realistic 3D images of the urban fabric under various flooding scenarios (Macchione et al., 2019b; Wang et al., 2019; Costabile et al., 2021). Moreover, the calculation results are more and more communicated through web services (Shen et al., 2020; Heyer et al., 2020). Nonetheless, as recently highlighted by Rosenzweig et al. (2021), further efforts should be dedicated to bridge the gaps between advances in hydrodynamic modelling and their transfer towards improved studies by water managers and engineering offices.

Declaration of Competing Interest

The authors declare that they have no known competing financial interests or personal relationships that could have appeared to influence the work reported in this paper.

References

Anni, A.H., Cohen, S., Praskievicz, S., 2020. Sensitivity of urban flood simulations to stormwater infrastructure and soil infiltration. J. Hydrol. 588, 125028.
Arrault, A., Finaud-Guyot, P., Archambeau, P., Bruwier, M., Erpicum, S., Pirotton, M., Dewals, B., 2016. Hydrodynamics of long-duration urban floods: experiments and numerical modelling. Nat. Hazards Earth Syst. Sci. 16 (6), 1413–1429.
Arrighi, C., Campo, L., 2019. Effects of digital terrain model uncertainties on high-resolution urban flood damage assessment. J. Flood Risk Manage. 12 (S2), e12530.
Baba, Y., Ishigaki, T., Toda, K., 2017. Experimental studies on safety evacuation from underground spaces under inundation situations. J. JSCE 5 (1), 269–278.
Bates, P.D., 2022. Flood inundation prediction. Annu. Rev. Fluid Mech. 54, 287–315.
Beg, M.N.A., Rubinato, M., Carvalho, R.F., Shucksmith, J.D., 2020. CFD modelling of the transport of soluble pollutants from sewer networks to surface flows during urban flood events. Water 12 (9), 2514.
Berkhahn, S., Fuchs, L., Neuweiler, I., 2019. An ensemble neural network model for real-time prediction of urban floods. J. Hydrol. 575, 743–754.
Bermúdez, M., Zischg, A.P., 2018. Sensitivity of flood loss estimates to building representation and flow depth attribution methods in micro-scale flood modelling. Nat. Hazards 92 (3), 1633–1648.
Bermúdez, M., Ntegeka, V., Wolfs, V., Willems, P., 2018. Development and comparison of two fast surrogate models for urban pluvial flood simulations. Water Resour. Manage. 32 (8), 2801–2815.
Bernardini, G., Quagliarini, E., D'Orazio, M., Brocchini, M., 2020. Towards the simulation of flood evacuation in urban scenarios: Experiments to estimate human motion speed in floodwaters. Saf. Sci. 123, 104563.
Bocanegra, R.A., Vallés-Morán, F.J., Francés, F., 2020. Review and analysis of vehicle stability models during floods and proposal for future improvements. J. Flood Risk Manage. 13, e12551.
Braschi G., Gallati M., Natale L., 1989. Simulation of a road network flooding, *Conference on Modeling and Simulation, Pittsburgh*, 8 pages.

Brunner, M.I., Slater, L., Tallaksen, L.M., Clark, M., 2021. Challenges in modelling and predicting floods and droughts: a review. Wiley Interdisciplinary Reviews: Water 8 (3), e1520.
Bruwier, M., Mustafa, A., Aliaga, D.G., Archambeau, P., Erpicum, S., Nishida, G., Dewals, B., 2018. Influence of urban pattern on inundation flow in floodplains of lowland rivers. Sci. Total Environ. 622, 446–458.
Bruwier, M., Maravat, C., Mustafa, A., Teller, J., Pirotton, M., Erpicum, S., Dewals, B., 2020. Influence of urban forms on surface flow in urban pluvial flooding. J. Hydrol. 582, 124493.
Bulti, D.T., Abebe, B.G., 2020. A review of flood modelling methods for urban pluvial flood application. Model. Earth Syst. Environ. 6 (3), 1293–1302.
Chang, T.J., Wang, C.H., Chen, A.S., Djordjević, S., 2018. The effect of inclusion of inlets in dual drainage modelling. J. Hydrol. 559, 541–555.
Chanson, H., Brown, R., 2018. Stability of individuals during urban inundations: what should we learn from field observations? Geosciences 8 (9), 341.
Chen, A.S., Evans, B., Djordjević, S., Savić, D.A., 2012. A coarse-grid approach to representing building blockage effects in 2D urban flood modelling. J. Hydrol. 426, 1–16.
Chen, S., Garambois, P.A., Finaud-Guyot, P., Dellinger, G., Mose, R., Terfous, A., Ghenaim, A., 2018. Variance based sensitivity analysis of 1D and 2D hydraulic models: an experimental urban flood case. Environ. Modell. Software 109, 167–181.
Chibane, T., Paquier, A., Benmamar, S., 2018. Coupled 1D/2D Hydraulic Simulation of the Model Muri. In: Gourbesville, P., Cunge, J., Caignaert, G. (Eds.), Advances in Hydroinformatics. Springer Water, Springer, Singapore.
Chibane, T., Paquier, A., Benmamar, S., 2021. Experimental study of the flow patterns in a street during drainage or overflow to or from drains. Urban Water J. 18 (7), 544–557.
Contreras, M.T., Gironás, J., Escauriaza, C., 2020. Forecasting flood hazards in real time: a surrogate model for hydrometeorological events in an Andean watershed. Nat. Hazards Earth Syst. Sci. 20 (12), 3261–3277.
Costabile, P., Costanzo, C., De Lorenzo, G., Macchione, F., 2020. Is local flood hazard assessment in urban areas significantly influenced by the physical complexity of the hydrodynamic inundation model? J. Hydrol. 580, 124231.
Costabile, P., Costanzo, C., De Lorenzo, G., De Santis, R., Penna, N., Macchione, F., 2021. Terrestrial and airborne laser scanning and 2-D modelling for 3-D flood hazard maps in urban areas: new opportunities and perspectives. Environ. Modell. Software 135, 104889.
Darabi, H., Choubin, B., Rahmati, O., Haghighi, A.T., Pradhan, B., Kløve, B., 2019. Urban flood risk mapping using the GARP and QUEST models: a comparative study of machine learning techniques. J. Hydrol. 569, 142–154.
Darabi, H., Haghighi, A.T., Mohamadi, M.A., Rashidpour, M., Ziegler, A.D., Hekmatzadeh, A.A., Kløve, B., 2020. Urban flood risk mapping using data-driven geospatial techniques for a flood-prone case area in Iran. Hydrol. Res. 51 (1), 127–142.
de Almeida, G.A., Bates, P., Ozdemir, H., 2018. Modelling urban floods at submetre resolution: challenges or opportunities for flood risk management? J. Flood Risk Manage. 11, S855–S865.
Dewals, B., Bruwier, M., Pirotton, M., Erpicum, S., Archambeau, P., 2021. Porosity models for large-scale urban flood modelling: a review. Water 13 (7), 960.
Djordjevic, S., Prodanovic, D., Maksimovic, C., 1999. An approach to simulation of dual drainage. Water Sci. Technol. 39 (9), 95–103.
Dong, B., Xia, J., Zhou, M., Deng, S., Ahmadian, R., Falconer, R.A., 2021. Experimental and numerical model studies on flash flood inundation processes over a typical urban street. Adv. Water Resour. 147, 103824.
EEA, 2019. Economic Lossess from Climate-Related Extremes in Europe. Indicator Assessment. https://www.eea.europa.eu/data-and-maps/indicators/river-floods-3/assessment.
Feng, B., Wang, J., Zhang, Y., Hall, B., Zeng, C., 2020. Urban flood hazard mapping using a hydraulic–GIS combined model. Nat. Hazards 100 (3), 1089–1104.
Fernández-Pato, J., García-Navarro, P., 2021. An efficient GPU implementation of a coupled overland-sewer hydraulic model with pollutant transport. Hydrology 8, 146.
Ferrari, A., Viero, D.P., 2020. Floodwater pathways in urban areas: a method to compute porosity fields for anisotropic subgrid models in differential form. J. Hydrol. 589, 125193.
Ferrari, A., Viero, D.P., Vacondio, R., Defina, A., Mignosa, P., 2019. Flood inundation modeling in urbanized areas: a mesh-independent porosity approach with anisotropic friction. Adv. Water Resour. 125, 98–113.
Finaud-Guyot, P., Garambois, P.A., Araud, Q., Lawniczak, F., François, P., Vazquez, J., Mosé, R., 2018. Experimental insight for flood flow repartition in urban areas. Urban Water J. 15 (3), 242–250.
Finaud-Guyot, P., Garambois, P.A., Dellinger, G., Lawniczak, F., François, P., 2019. Experimental characterization of various scale hydraulic signatures in a flooded branched street network. Urban Water J. 16 (9), 609–624.
Fowdar, H., Payne, E., Schang, C., Zhang, K., Deletic, A., McCarthy, D., 2021. How well do stormwater green infrastructure respond to changing climatic conditions? J. Hydrol. 603, 126887.
Geng, Y., Zhu, B., Zheng, X., 2020. Effect of independent variables on urban flood models. Water 12 (12), 3442.
Geuzaine, C., Remacle, J.F., 2009. Gmsh: a 3-D finite element mesh generator with built-in pre-and post-processing facilities. Int. J. Numer. Meth. Eng. 79 (11), 1309–1331.
Gómez, M., Russo, B., Tellez-Alvarez, J., 2019. Experimental investigation to estimate the discharge coefficient of a grate inlet under surcharge conditions. Urban Water J. 16 (2), 85–91.
Guinot, V., Soares-Frazão, S., 2006. Flux and source term discretization in two-dimensional shallow water models with porosity on unstructured grids. Int. J. Numerical Methods Fluids 50, 309–345.
Guinot, V., Sanders, B.F., Schubert, J.E., 2017. Dual integral porosity shallow water model for urban flood modelling. Adv. Water Resour. 103, 16–31.
Guinot, V., Delenne, C., Rousseau, A., Boutron, O., 2018. Flux closures and source term models for shallow water models with depth-dependent integral porosity. Adv. Water Resour. 122, 1–26.
Güney, M.S., Tayfur, G., Bombar, G., Elci, S., 2014. Distorted physical model to study sudden partial dam break flows in an urban area. J. Hydraul. Eng. 140 (11), 05014006.
Guo, K., Guan, M., Yu, D., 2021a. Urban surface water flood modelling–a comprehensive review of current models and future challenges. Hydrol. Earth Syst. Sci. 25 (5), 2843–2860.
Guo, Z., Leitao, J.P., Simões, N.E., Moosavi, V., 2021b. Data-driven flood emulation: speeding up urban flood predictions by deep convolutional neural networks. J. Flood Risk Manag 14, 12684.
Haltas, I., Tayfur, G., Elci, S., 2016a. Two-dimensional numerical modeling of flood wave propagation in an urban area due to Ürkmez dam-break, İzmir, Turkey. *Nat. Hazards* 81 (3), 2103–2119.
Haltas, I., Elçi, S., Tayfur, G., 2016b. Numerical simulation of flood wave propagation in two-dimensions in densely populated urban areas due to dam break. Water Resour. Manage. 30 (15), 5699–5721.
Hao, X., Li, Y., Liu, S., 2021. Comparison of dynamic flow interaction methods between pipe system and overland in urban flood analysis. Sci. Rep. 11 (1), 1–17.
Heping H., Jianzhong G., Yi Shen., 1999. An urban flood dynamic simulation model with GIS, *28th IAHR Conference, Graz, Austria*.
Heyer, T., Hammoudi, H., Zimmermann, R., Backhaus, L., Stamm, J., Schilling, A., St, T., 2020. Flood risk analysis and communication using digital twins of urban areas. Proceedings of the 10th Conference on Fluvial Hydraulics (Delft.
Hirabayashi, Y., Mahendran, R., Koirala, S., Konoshima, L., Yamazaki, D., Watanabe, S., Kanae, S., 2013. Global flood risk under climate change. Nat. Clim. Change 3 (9), 816–821.
Hu, R., Fang, F., Salinas, P., Pain, C.C., 2018. Unstructured mesh adaptivity for urban flooding modelling. J. Hydrol. 560, 354–363.
Jang, J.H., Chang, T.H., Chen, W.B., 2018. Effect of inlet modelling on surface drainage in coupled urban flood simulation. J. Hydrol. 562, 168–180.
Jang, J.H., Hsieh, C.T., Chang, T.H., 2019. The importance of gully flow modelling to urban flood simulation. Urban Water J. 16 (5), 377–388.
Kankanamge, N., Yigitcanlar, T., Goonetilleke, A., Kamruzzaman, M., 2020. Determining disaster severity through social media analysis: Testing the methodology with South East Queensland Flood tweets. Int. J. Disaster Risk Reduct. 42, 101360.
Kemper, S., Schlenkhoff, A., 2019. Experimental study on the hydraulic capacity of grate inlets with supercritical surface flow conditions. Water Sci. Technol. 79 (9), 1717–1726.
Kim, H.I., Han, K.Y., 2020. Urban flood prediction using deep neural network with data augmentation. Water 12 (3), 899.
Kim, H.I., Keum, H.J., Han, K.Y., 2019. Real-time urban inundation prediction combining hydraulic and probabilistic methods. Water 11 (2), 293.
Kinoshita S., Sate S., Terayama H., 1996. Flood simulation by two dimensional tank model, *7th Conference on Urban Storm Drainage, Hannover, Germany*: pp 959-964.
Kwon, S.-H., Kim, J.-H., 2021. Machine learning and urban drainage systems: state-of-the-art review. Water 13, 3545.
Kvocka, D., Falconer, R.A., Bray, M., 2016. Flood hazard assessment for extreme flood events. Nat. Hazards 84 (3), 1569–1599.
Le Coz, J., Patalano, A., Collins, D., Guillén, N.F., García, C.M., Smart, G.M., Braud, I., 2016. Crowdsourced data for flood hydrology: feedback from recent citizen science projects in Argentina, France and New Zealand. J. Hydrol. 541, 766–777.
Lei, X., Chen, W., Panahi, M., Falah, F., Rahmati, O., Uuemaa, E., Kalantari, Z., Ferreira, C., Rezai, F., Tiefenbacher, J.P., Lee, S., Bian, H., 2021. Urban flood modeling using deep-learning approaches in Seoul, South Korea. J. Hydrol. 601, 126684.
Leitão, J.P., de Sousa, L.M., 2018. Towards the optimal fusion of high-resolution Digital Elevation Models for detailed urban flood assessment. J. Hydrol. 561, 651–661.
Li, X., Erpicum, S., Bruwier, M., Mignot, E., Finaud-Guyot, P., Archambeau, P., Dewals, B., 2019. Laboratory modelling of urban flooding: strengths and challenges of distorted scale models. Hydrol. Earth Syst. Sci. 23 (3), 1567–1580.
Li, X., Erpicum, S., Mignot, E., Archambeau, P., Rivière, N., Pirotton, M., & Dewals, B. (2020). Numerical insights into the effects of model geometric distortion in laboratory experiments of urban flooding. *Water Resour. Res. 56*(7), e2019WR026774.
Li, X., Kitsikoudis, V., Mignot, E., Archambeau, P., Pirotton, M., Dewals, B., Erpicum, S. (2021). Experimental and numerical study of the effect of model geometric distortion on laboratory modeling of urban flooding. *Water Resour. Res.*, *57*(10), e2021WR029666.
Liu, L., Sun, J., Lin, B., Lu, L., 2018. Building performance in dam-break flow – an experimental study. Urban Water J. 15 (3), 251–258.
Macchione, F., Costabile, P., Costanzo, C., De Lorenzo, G., 2019a. Extracting quantitative data from non-conventional information for the hydraulic reconstruction of past urban flood events. A case study. *J. Hydrol.* 576, 443–465.
Macchione, F., Costabile, P., Costanzo, C., De Santis, R., 2019b. Moving to 3-D flood hazard maps for enhancing risk communication. Environ. Modell. Software 111, 510–522.
McMillan, H.K., Brasington, J. (2007). Reduced complexity strategies for modelling urban floodplain inundation. *Geomorphology* 90, 226–243.
Martínez-Gomariz, E., Gómez, M., Russo, B., 2016. Experimental study of the stability of pedestrians exposed to urban pluvial flooding. Nat. Hazards 82 (2), 1259–1278.

Martínez-Gomariz, E., Gómez, M., Russo, B., Djordjević, S., 2017. A new experiments-based methodology to define the stability threshold for any vehicle exposed to flooding. Urban Water J. 14 (9), 930–939.
Martínez-Gomariz, E., Gómez, M., Russo, B., Djordjević, S., 2018. Stability criteria for flooded vehicles: a state-of-the-art review. J. Flood Risk Manage. 11, S817–S826.
Martínez-Gomariz, E., Russo, B., Gómez, M., Plumed, A., 2020. An approach to the modelling of stability of waste containers during urban flooding. J. Flood Risk Manage. 13, e12558.
Martins, R., Leandro, J., Djordjević, S., 2018a. Influence of sewer network models on urban flood damage assessment based on coupled 1D/2D models. J. Flood Risk Manage. 11, S717–S728.
Martins, R., Rubinato, M., Kesserwani, G., Leandro, J., Djordjević, S., Shucksmith, J.D., 2018b. On the characteristics of velocities fields in the vicinity of manhole inlet grates during flood events. Water Resour. Res. 54 (9), 6408–6422.
Mei, C., Liu, J., Wang, H., Li, Z., Yang, Z., Shao, W., Yan, D., 2020. Urban flood inundation and damage assessment based on numerical simulations of design rainstorms with different characteristics. Sci. China Technol. Sci. 63 (11), 2292–2304.
Mejía-Morales, M.A., Mignot, E., Paquier, A., Sigaud, D., Proust, S., 2021. Impact of the porosity of an urban block on the flood risk assessment: a laboratory experiment. J. Hydrol. 602, 126715.
Mignot, E., Camusson, L., Riviere, N., 2020. Measuring the flow intrusion towards building areas during urban floods: impact of the obstacles located in the streets and on the facade. J. Hydrol. 583, 124607.
Mignot, E., Li, X., Dewals, B., 2019. Experimental modelling of urban flooding: a review. J. Hydrol. 568, 334–342.
Molinari, D., De Bruijn, K.M., Castillo-Rodríguez, J.T., Aronica, G.T., Bouwer, L.M., 2019. Validation of flood risk models: current practice and possible improvements. Int. J. Disaster Risk Reduct. 33, 441–448.
Moy de Vitry, M., Kramer, S., Wegner, J.D., Leitão, J.P., 2019. Scalable flood level trend monitoring with surveillance cameras using a deep convolutional neural network. Hydrol. Earth Syst. Sci. 23 (11), 4621–4634.
Mustafa, A., Szydłowski, M., 2021. Application of different building representation techniques in HEC-RAS 2-D for urban flood modeling using the Toce River experimental case. PeerJ 9, e11667.
Nania, L.S., 1999. Metodologia numérico-experimental para el analisis del riesgo asociado a la escorrentia pluvial en una red de calles. PhD thesis. Universitat politècnica de Catalunya, Barcelona.
Nkwunonwo, U.C., Whitworth, M., Baily, B., 2020. A review of the current status of flood modelling for urban flood risk management in the developing countries. Sci. African 7, e00269.
Paquier, A., Bazin, P.H., El Kadi Abderrezzak, K., 2020. Sensitivity of 2D hydrodynamic modelling of urban floods to the forcing inputs: lessons from two field cases. Urban Water J. 17 (5), 457–466.
Postacchini, M., Bernardini, G., D'Orazio, M., Quagliarini, E., 2021. Human stability during floods: experimental tests on a physical model simulating human body. Saf. Sci. 137, 105153.
Quintana-Romero, T., Leandro, J., 2021. A method to devise multiple model structures for urban flood inundation uncertainty. J. Hydrol. 127246.
Ramsauer, S., Leandro, J., Lin, Q., 2021. Inclusion of narrow flow paths between buildings in coarser grids for urban flood modeling: virtual surface links. Water 13 (19), 2629.
Rong, Y., Zhang, T., Zheng, Y., Hu, C., Peng, L., Feng, P., 2020. Three-dimensional urban flood inundation simulation based on digital aerial photogrammetry. J. Hydrol. 584, 124308.
Rosenzweig, B. R., Herreros Cantis, P., Kim, Y., Cohn, A., Grove, K., Brock, J., ... & Chang, H. (2021). The value of urban flood modeling. *Earth's Fut.* 9(1), e2020EF001739.
Rözer, V., Peche, A., Berkhahn, S., Feng, Y., Fuchs, L., Graf, T., et al. (2021). Impact-based forecasting for pluvial floods. *Earth's Fut.*, 9, e2020EF001851.
Rubinato, M., Lashford, C., Goerke, M., 2020. Advances in experimental modelling of urban flooding. In: Water-wise cities and sustainable water systems, p. 235.
Rubinato, M., Lee, S., Martins, R., Shucksmith, J.D., 2018a. Surface to sewer flow exchange through circular inlets during urban flood conditions. J. Hydroinf. 20 (3), 564–576.
Rubinato, M., Martins, R., Shucksmith, J.D., 2018b. Quantification of energy losses at a surcharging manhole. Urban Water J. 15 (3), 234–241.
Rubinato, M., Helms, L., Vanderlinden, M., Hart, J., Martins, R., 2021. Flow exchange, energy losses and pollutant transport in a surcharging manhole linked to street profiles. J. Hydrol. 127201.
Sämann, R., Graf, T., Neuweiler, I., 2019. Modeling of contaminant transport during an urban pluvial flood event–the importance of surface flow. J. Hydrol. 568, 301–310.
Sanders, B.F., Schubert, J.E., Gallegos, H.A., 2008. Integral formulation of shallow-water equations with anisotropic porosity for urban flood modeling. J. Hydrol. 362, 19–38.
Schubert, J.E., Sanders, B.F., 2012. Building treatments for urban flood inundation models and implications for predictive skill and modeling efficiency. Adv. Water Resour. 41, 49–64.
Scotti, V., Giannini, M., Cioffi, F., 2020. Enhanced flood mapping using synthetic aperture radar (SAR) images, hydraulic modelling, and social media: a case study of Hurricane Harvey (Houston, TX). J. Flood Risk Manage. 13 (4), e12647.
Seong, H., Rhee, D.S., Park, I., 2020. Analysis of urban flood inundation patterns according to rainfall intensity using a rainfall simulator in the Sadang Area of South Korea. Appl. Sci. 10 (3), 1158.
Shen, J., Tan, F., 2020. Effects of DEM resolution and resampling technique on building treatment for urban inundation modeling: a case study for the 2016 flooding of the HUST campus in Wuhan. Nat. Hazards 104 (1), 927–957.
Shen, J., Tan, F., Zhang, Y., 2018. Improved building treatment approach for urban inundation modeling: a case study in Wuhan, China. *Water* 10 (12), 1760.
Shen, J., Zhou, J., Zhou, J., Herman, L., Reznik, T., 2020. Constructing the CityGML ADE for the Multi-Source Data Integration of Urban Flooding. ISPRS Int. J. Geo-Inf. 9 (6), 359.
Smith, G.P., Rahman, P.F., Wasko, C., 2016. A comprehensive urban floodplain dataset for model benchmarking. Int. J. River Basin Manage. 14 (3), 345–356.
Smith, G.P., Modra, B.D., Felder, S., 2019. Full-scale testing of stability curves for vehicles in flood waters. J. Flood Risk Manage. 12 (S2), e12527.
Sturm, M., Gems, B., Keller, F., Mazzorana, B., Fuchs, S., Papathoma-Köhle, M., Aufleger, M., 2018. Experimental analyses of impact forces on buildings exposed to fluvial hazards. J. Hydrol. 565, 1–13.
Varra, G., Pepe, V., Cimorelli, L., Della Morte, R., Cozzolino, L., 2020. On integral and differential porosity models for urban flooding simulation. Adv. Water Resour. 136, 103455.
Viero, D.P., 2019. Modelling urban floods using a finite element staggered scheme with an anisotropic dual porosity model. J. Hydrol. 568, 247–259.
Wang, C., Hou, J., Miller, D., Brown, I., Jiang, Y., 2019. Flood risk management in sponge cities: the role of integrated simulation and 3D visualization. Int. J. Disaster Risk Reduct. 39, 101139.
Wang, P., Li, Y., Yu, P., Zhang, Y., 2021. The analysis of urban flood risk propagation based on the modified Susceptible Infected Recovered model. J. Hydrol. 603, 127121.
Wu, Z., Zhou, Y., Wang, H., Jiang, Z., 2020. Depth prediction of urban flood under different rainfall return periods based on deep learning and data warehouse. Sci. Total Environ. 716, 137077.
Xing, Y., Liang, Q., Wang, G., Ming, X., Xia, X., 2019. City-scale hydrodynamic modelling of urban flash floods: the issues of scale and resolution. Nat. Hazards 96 (1), 473–496.
Yalcin, E., 2020. Assessing the impact of topography and land cover data resolutions on two-dimensional HEC-RAS hydrodynamic model simulations for urban flood hazard analysis. Nat. Hazards 101 (3), 995–1017.
Zhang, Y., Chen, Z., Zheng, X., Chen, N., Wang, Y., 2021a. Extracting the location of flooding events in urban systems and analyzing the semantic risk using social sensing data. J. Hydrol. 603, 127053.
Zhang, H., Wu, W., Hu, C., Hu, C., Li, M., Hao, X., Liu, S., 2021b. A distributed hydrodynamic model for urban storm flood risk assessment. J. Hydrol. 600, 126513.
Zhou, Q., Yu, W., Chen, A.S., Jiang, C., Fu, G., 2016. Experimental assessment of building blockage effects in a simplified urban district. Procedia Eng. 154, 844–852.